PAPER

# A scanning-free wide-field single-fiber endoscopic image retrieval method based on optical transmission matrix

IOP Publishing | Astro Ltd Laser Physics

Laser Phys. **29** (2019) 046202 (5pp) https://doi.org/10.1088/1555-6611/ab0365

# A scanning-free wide-field single-fiber endoscopic image retrieval method based on optical transmission matrix

**Chengfang Xu[1,2,3], Bin Zhuang[1,3], Yi Geng[1,3], Hui Chen[1,3], Liyong Ren[1] and Zhaoxin Wu[2]**

[1] Research Department of Information Photonics, Xi'an Institute of Optics and Precision Mechanics, Chinese Academy of Sciences, Xi'an 710119, People's Republic of China
[2] Department of Electronics Science and Technology, School of Electronic and Information Engineering, Xi'an Jiaotong University, Xi'an 710049, People's Republic of China
[3] University of Chinese Academy of Sciences, Beijing 100049, People's Republic of China

E-mail: renliy@opt.ac.cn

Received 29 November 2018
Accepted for publication 23 January 2019
Published 6 March 2019


**Abstract**

Light waves transmitting in a multimode optical fiber (MMF) for endoscopic imaging, due to modal dispersion, inevitably suffer two severe distortions: on the way in for illuminating and on the way out for imaging, which becomes a big challenge when using a single MMF for endoscopic applications. In this paper, based on obtaining the optical transmission matrix of the MMF working in the endoscopic mode, we propose a new method for retrieving endoscopic images from speckle fields, where the two distortions could be eliminated simultaneously. Our experimental results demonstrate that the object images can be well reconstructed directly from distorted waves. In addition, no scanning operation is required when collecting images, which is timesaving. Such an efficient method might have potential applications for wide-field and ultrathin fiber endoscopic imaging.

Keywords: single-fiber imaging, transmission matrix, endoscopic imaging, coherence imaging, computational imaging

(Some figures may appear in colour only in the online journal)

## 1. Introduction

Endoscope, a vital device for obtaining images of living organisms deep inside the body, is an important tool for biomedical imaging [1]. However, the diameters of typical commercial endoscopes (e.g. fiber bundles and/or GRIN lenses) are a few millimeters [2], which may lead to much invasive damage during imaging. It is urged to exploit an imaging system where optical elements with much smaller diameters are used for transmitting images. Fortunately, the single multimode optical fiber (MMF) is found to be a promising medium for endoscopic imaging, due to the advantages of its numerous transmission modes, small cross section, high pixel density and blind pixels free. However, using MMF for endoscopic imaging, the light wave transmitting in it always experiences two severe distortions: on the way in for illuminating and on the way out for imaging [3]. Therefore, such an inherent drawback becomes a fatal problem, and effective techniques must be developed to eliminate these distortions of the MMF before it can be actually used as a standalone endoscopic imaging device.

In fact, many methods have been proposed recently as for the endoscopic imaging applications using MMF [4–17]. These methods can be classified into two main types. One is the spot-scanning method (so-called the localized-sampling method), the other is the wide-field imaging method. The spot-scanning method, which includes the wavefront shaping method [4–11], the digital phase conjugation method [12–16] and the optical transmission matrix (TM) method [18, 19], has been verified to be capable of controlling the light waves

 

propagation in MMF and eliminating the distortion on the way in for illuminating. The working principle or process of the spot-scanning method can be described as follows. Firstly, the input light waves are modulated by either the spatial light modulator (SLM) or other optical field modulation devices and then are coupled to the MMF. Subsequently, a focused light spot is generated at the distal end (with respect to the light source) of the fiber, which is used to sample the object closing to the MMF tip. Finally, the reflected light from the sampled spot of the object goes back into the MMF, and the image of the object is acquired by scanning spot [20]. Note that, although no mechanical scanning operation is involved in the spot-scanning method, there exists an inherent disadvantage of slow speed due to the optical scanning operation realized by the complicated modulations to the optical fields. In addition, many methods have been proposed to overcome this disadvantage [21–26].

As for the wide-field imaging methods, a typical one among them is the lensless microendoscopy by a single fiber (LMSF) based on the angle-dependent optical TM method [3, 27, 28]. This LMSF method relies on modeling the MMF as a linear system, and by measuring the output optical field response to each input optical plane wave with different incident angle upon the MMF, the transmission characteristics of light in the MMF are established and stored in the TM. Using the TM obtained and making a reversal calculation from the output image, one can eliminate the on-the-way-out distortion and reconstruct the input image (i.e. the object). However, such a reconstructed image is still a speckle one due to the on-the-way-in distortion that always exists in the case of the endoscopic imaging. To further eliminate the on-the-way-in distortion and thus obtain a clean object image, two steps are applied. Firstly, during the process of imaging, the angle of incident light at the proximal end (with respect to the light source) of the fiber is scanned and the reconstructed speckle images corresponding to each incident angle are obtained; secondly, by averaging all the reconstructed speckle images, one can obtain a clean object image. Note that, although no mechanical scanning operation on the distal end of the fiber is used, a similar operation on the incident light is actually involved on the proximal end of it.

Apparently, the scanning operation is an unavoidable step in those methods, which consumes massive time during collecting images [3, 7, 13]. In this paper, we propose a novel MMF-based wide-field endoscopic imaging method to avoid scanning operation and to reduce image acquisition time. In our method, we introduce a new way to measure the optical TM of the MMF in the endoscopic mode since the traditional one-way optical TM becomes out of work in the endoscopic imaging. Our method can simultaneously eliminate the two distortions induced by the MMF. Experimental results indicate that the object can be reconstructed efficiently using only one distorted image of it, without involving any scanning operation during the process of image capture. It is envisaged that this efficient method may extend to more potential applications, such as wide-field and ultrathin fiber endoscopic imaging.

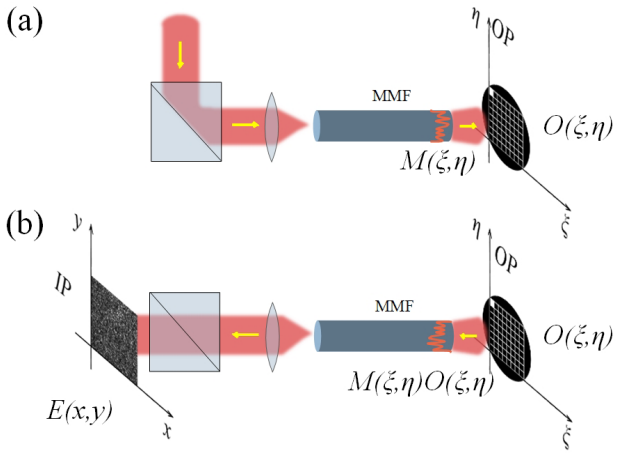


**Figure 1.** Schematic of the endoscopic imaging system based on the MMF. (a) The way in where a plane wave propagates through the MMF and generates a speckle field $M(\xi, \eta)$ at the object plane (OP); (b) the way out where the speckle field is reflected by the object $O(\xi, \eta)$ and then coupled into the MMF again. The output optical field $E(x, y)$ is detected at the image plane (IP).

## 2. Principle

Figure 1 shows the schematic of the MMF-based endoscopic imaging. Firstly, as shown in figure 1(a), the linearly polarized plane wave is focused by a lens and propagates through the MMF and generates a speckle field $M(\xi, \eta)$ at the object plane (OP), which is used for illumination. However, the precise speckle field of the $M(\xi, \eta)$ is unknown due to the on-the-way-in distortion by the MMF. Secondly, as shown in figure 1(b), the speckle field is reflected by the object and then the modulated speckle field, $M(\xi, \eta) * O(\xi, \eta)$, is coupled into the same MMF. Here the '$*$' denotes a multiplication operation based on elements according to the coordinates of $(\xi, \eta)$. Note that, this modulated speckle field contains the information of the object (represented by $O(\xi, \eta)$) and will be distorted again by the MMF. Thus, in the MMF-based endoscopic imaging system, $O(\xi, \eta)$ is distorted twice. Finally, the output speckle field $E(x, y)$ is recorded at the image plane (IP). In this paper, our main work is to recover $O(\xi, \eta)$ from $E(x, y)$ by eliminating the two distortions.

The MMF is a kind of complex medium in optics due to modal dispersion. For imaging through complex medium, the traditional one-way optical TM approach is proposed by Popoff *et al* [29, 30], where a linearly polarized plane wave is used for illumination. The light wave is modulated by the object and then transmits through the complex medium, thus it is distorted once by the complex medium, and the measured TM actually only involves the one-way distortion (from the OP to the image plane). Different from [29], in the MMF-based endoscopic imaging system, not only the output optical field is distorted (from the OP to the image plane), but also the illumination light is distorted to a speckle field $M(\xi, \eta)$. In this case, the output speckle field can be written as

$$E(x,y) = \sum_{(\xi,\eta)} K(x,y;\xi,\eta) * [M(\xi,\eta) * O(\xi,\eta)], \quad (1)$$

where $K(x, y; \xi, \eta)$ is the traditional one-way TM of the MMF, which represents the relationship between the reflected speckle field $M(\xi, \eta) * O(\xi, \eta)$ and the output speckle field $E(x, y)$. The $M(\xi, \eta) * O(\xi, \eta)$ can be measured once one obtains $E(x, y)$ by using the traditional one-way TM. However, during endoscopic imaging, one cannot recover the object $O(\xi, \eta)$ since illumination optical field $M(\xi, \eta)$ is unknown.

To solve this problem, we need to measure the optical TM $T(x, y; \xi, \eta)$ of the endoscopic imaging system, which contains two distortions involved and can be expressed by

$$T(x, y; \xi, \eta) = K(x, y; \xi, \eta) * M(\xi, \eta). \tag{2}$$

Thus, equation (1) can be rewritten as

$$E(x, y) = \sum_{(\xi,\eta)} T(x, y; \xi, \eta) * O(\xi, \eta). \tag{3}$$

It is seen from equations (1) and (3) that, although illumination speckle field $M(\xi, \eta)$ is unknown, the object $O(\xi, \eta)$ can be recovered by using the measured $T(x, y; \xi, \eta)$ which contains the information of $M(\xi, \eta)$.

Furthermore, for the convenience of calculation, the equation (3) is converted to the matrix form as

$$E = T \times O, \tag{4}$$

where '$\times$' denotes the multiplication operation between two matrices. The more detailed about data conversion will be shown in section 4. Once $T$ and $E$ are measured, $O$ can be constructed directly from $E$ by using the inversion matrix method

$$O = T^{-1} \times E, \tag{5}$$

where $T^{-1}$ represents the inversion of the optical TM.

It should be pointed out that both $E$ and $O$ are the complex amplitude of the optical field, and, by introducing a reference light to yield an interference image, $E$ can be measured by using the phase-shifting digital holography technology [31].

## 3. Experimental setup

The endoscopic imaging system is shown in figure 2. The light wave emitted from a He–Ne laser ($\lambda = 632.8$ nm) is expanded by a beam expander (BE), polarized by a linear polarizer (P1), and split into two beams by a beam splitter (BS). One beam, as the reference beam, is reflected by the SLM. The other beam, as the object beam, is initially coupled to the MMF by an objective lens, guided by the MMF and delivered to the OP. At the OP, we use a digital micromirror device (DMD) to modulate the optical field. Then, after being reflected by the object, it is coupled back into the MMF again and transmits towards the IP through the MMF. Finally, the object beam and the reference beam combines at the BS to form an interference image at the CMOS camera.

The SLM is utilized to realize the phase-shift for the phase-shifting digital holography, in fact, any other phase shifters, such as the piezoelectric transducer driven mirror and the acousto-optic modulator, can replace it. Using of SLM, the liquid crystal array allows faster switching time and better stability. In our experiment, we use a step-index polymer optical fiber (POF) with a length of 0.5 m. Generally, comparing with glass optical fibers (GOFs), POFs provide higher elastic strain range, fracture toughness and flexibility. Therefore, they are good candidates since they are much safer inside the organism.

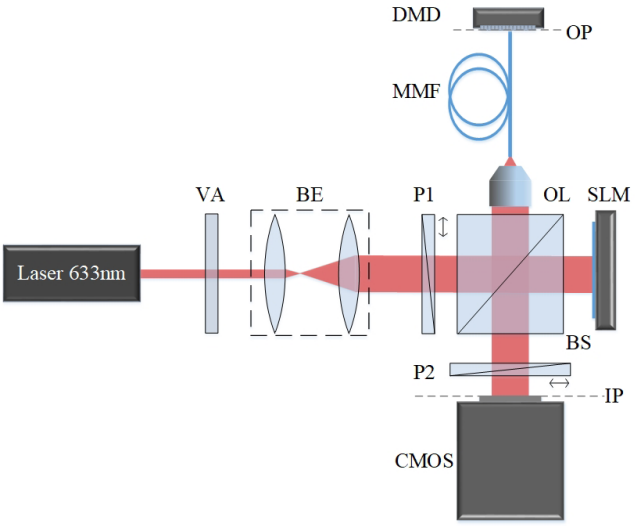


**Figure 2.** Setup for endoscopic imaging by using a single MMF. The interference between the object beam (reflected by the DMD located clearly at the end of the MMF) and the reference beam (reflected by SLM) is recorded by a CMOS. VA: variable attenuator. BE: beam expander. P1, P2: linear polarizer. BS: beam splitter. OL: objective lens. MMF: multimode optical fiber (polymer optical fiber, NA: 0.5; the diameter of the core: 980 $\mu$m; fiber length: 0.5 m). DMD: digital micromirror devices (ViALUX, V-7001VIS, the size of one pixel is 13.7 $\mu$m). SLM: the liquid-crystal spatial light modulator (Meadowlark Optics, P1920-0635-HDMI). CMOS: CMOS camera (Hamamatsu, C13440-20CU, the central 256 $\times$ 256 pixels are used for imaging).

## 4. Results and discussions

There are two steps in our proposed endoscopic imaging method. The first step is to measure the optical TM $T(x, y; \xi, \eta)$; the second step is to recover the object $O(\xi, \eta)$ using the $T(x, y; \xi, \eta)$ measured. In our experiment, we load a binary amplitude object onto the DMD as a target object. The object to be imaged, as the input channels with a size of 14 pixels $\times$ 12 pixels, is selected at the center of the DMD; while the imaging window, as the output channels with a size of 256 pixels $\times$ 256 pixels, is set at the center of the CMOS. We use $N$ and $M$ to denote the number of the input and the output channels, respectively. In this case, we have $N = 168$ and $M = 65\,536$.

Mathematically, the input channel (denoted by $n$) and the output channel (denoted by $m$) are determined by the coordinate $(\xi, \eta)$ at the OP and the coordinate $(x, y)$ at the IP, respectively, and they can be expressed by

$$\begin{cases} m = (y-1) * x_{max} + x \\ n = (\eta - 1) * \xi_{max} + \xi \end{cases}, \tag{6}$$

where $x_{max}$ and $\xi_{max}$ are the maximum values of $x$ and $\xi$, respectively.

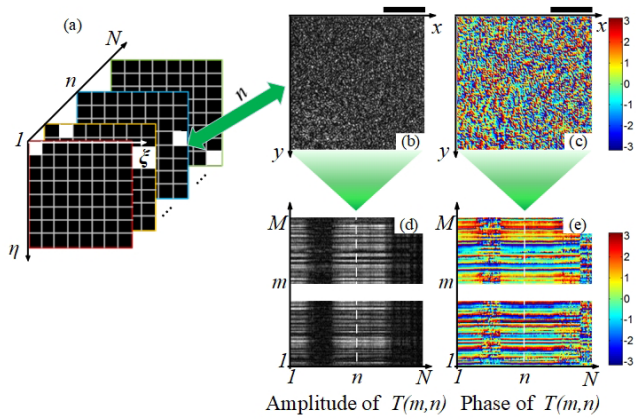


**Figure 3.** Measuring the optical TM $T(m, n)$. (a) The input channels are switched on in sequence. The amplitude (b) and the phase (c) of the output optical field related to the $n$th input channel, respectively; (d) and (e) are the amplitude and the phase of $T(m, n)$, respectively. All data in (b) and (c) are stored in the location of the white dotted lines in (d) and (e). $n$: the $n$th input channel. $m$: the $m$th output channel. $N$ and $M$ represent the number of the input and the output channels, respectively. Scale bars: 500 $\mu$m, color bar: phase in radian.

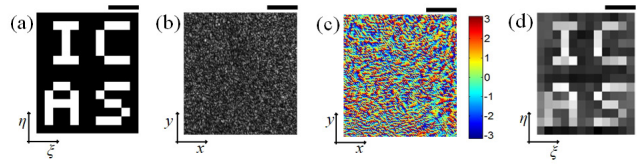


**Figure 4.** Reconstruction of the object image. (a) A binary amplitude object $O(\xi, \eta)$. (b) and (c) are the amplitude and the phase of the output optical field $E(x, y)$ of the object, respectively, with 256 pixels $*$ 256 pixels. (d) Reconstructed the object image $O_r(\xi, \eta)$. Scale bars indicate 50 $\mu$m in (a), (d) and 500 $\mu$m in (b), (c). Color bar: phase in radian. The correlation coefficient between (a) and (d) is 0.91.

With the help of the above definitions of $m$ and $n$, the optical TM $T(x, y; \xi, \eta)$ can be simplified to $T(m, n)$, which describes the optical response relationship between the $n$th input channel and the $m$th output channel.

Let us see how can we measure the $T(m, n)$ of the MMF. For this purpose, we switch on the $n$th input channel in sequence at the OP (as shown in figure 3(a)) and measure the optical field $E_n(x, y)$ at the IP accordingly. It should be pointed out that, in this process, the phase-shifting digital holography technology is used. The amplitude and the phase of $E_n(x, y)$ of all output channels when switching on the $n$th input channel are shown in figures 3(b) and (c), respectively. What's more, based on equation (6) and using $T(m, n) = E_n(x, y)$, a complete TM $T(m, n)$ can be constructed. Shown in figures 3(d) and (e) are the amplitude and the phase of TM $T(m, n)$, respectively. It is seen that figures 3(b) and (c) corresponding to the $n$th input channel become the white dotted lines in figures 3(d) and (e), respectively.

In what flows, let us see the validity of the proposed endoscopic imaging method. For this purpose, we load a binary amplitude object $O(\xi, \eta)$ onto the DMD where the reflectivity of the background and that of the characters are 0 and 1, respectively, as shown in figure 4(a). In this case, the output optical field $E(x, y)$ of the object can be obtained by using the phase-shifting digital holography technology again. Figures 4(b) and (c) are the amplitude and the phase of the output optical field $E(x, y)$, respectively. Obviously, they have been distorted seriously by the MMF.

To recover the object image, by using equation (6), the output optical field can be rewritten as

$$E_{1D}(m) = E(x, y), \tag{7}$$

where $E_{1D}(m)$ is the output optical field represented by the 1D array. Thus, using the optical TM $T(m, n)$ the information of the object can be obtained from $E_{1D}(m)$ by

$$O_{1D}(n) = T^{-1}(n, m) \times E_{1D}(m), \tag{8}$$

where $T^{-1}(n, m)$ is the inversion of the $T(m, n)$. Because the number of the input channels and that of the output channels are not equal, the inversion is extended with the pseudo inversion operation.

Again, by using equation (6), the reconstructed object, $O_r(\xi, \eta)$, can be reconstructed based on the following equation

$$O_r(\xi, \eta) = |O_{1D}(n)|. \tag{9}$$

The reconstructed object is shown in figure 4(d). To quantitatively describe the reliability of this method in information extraction, the correlation coefficient $R_s$ is introduced to represent the correlation of the object $O$ and the recovered object image $O_r$ by [32]

$$R_s = \frac{\mathrm{cov}(O, O_r)}{\sigma_O \sigma_{O_r}}, \tag{10}$$

where cov and $\sigma$ represent the covariance and the standard deviation, respectively. Calculation demonstrates that the correlation coefficient between figures 4(a) and (d) is 0.91, which indicates that most information of the object has been successfully recovered from the distorted output optical field. This proves that the optical TM measured in the endoscopic mode has the ability to eliminate the two distortions simultaneously and efficiently recover the object from one output optical field of the object. Besides, the experimental results demonstrate that our method has potential applications for MMF-based endoscopic imaging.

## 5. Conclusion

In conclusion, we propose a novel MMF-based wide-field endoscopic imaging method to avoid scanning and reduce image acquisition time during the process of image capture. The advantage of this method is that the two distortions of the optical field (on-the-way-in and on-the-way-out distortions) can be eliminated simultaneously when reconstructing the object. Experimental results demonstrate that, via the measured optical TM of the MMF, the image of the object can be reconstructed by using only one output speckle field of the object, without any scanning operations during the process of image capture. Compared with other single-fiber-based

endoscopic imaging methods, the time for collecting image information will be greatly reduced. Such an efficient method might have potential applications for wide-field and ultrathin fiber endoscopic imaging. However, we have only verified the feasibility of this method in the early stage. As for actual imaging, especially in biological tissues, the situation is more complicated and further research is needed.

## Acknowledgments

This work was supported by the National Natural Science Foundation of China under Grant No. 61535015.

## References

[1] Psaltis D and Moser C 2016 *Opt. Photonics News* **27** 24
[2] Caravaca-Aguirre A M and Piestun R 2017 *Opt. Express* **25** 1656
[3] Choi Y, Yoon C, Kim M, Yang T D, Fang-Yen C, Dasari R R, Lee K J and Choi W 2012 *Phys. Rev. Lett.* **109** 203901
[4] Di Leonardo R and Bianchi S 2011 *Opt. Express* **19** 247
[5] Cizmar T and Dholakia K 2011 *Opt. Express* **19** 18871
[6] Bianchi S and Di Leonardo R 2012 *Lab Chip* **12** 635
[7] Cizmar T and Dholakia K 2012 *Nat. Commun.* **3** 1027
[8] Amitonova L V, Descloux A, Petschulat J, Frosz M H, Ahmed G, Babic F, Jiang X, Mosk A P, Russell P S J and Pinkse P W H 2016 *Opt. Lett.* **41** 497
[9] Yin Z, Liu G, Chen F and Liu B 2015 *Chin. Opt. Lett.* **13** 071404
[10] Fan W, Hu X, Zhaxi B, Chen Z and Pu J 2018 *Opt. Express* **26** 7693
[11] Amphawan A 2012 *J. Mod. Opt.* **59** 460
[12] Papadopoulos I N, Farahi S, Moser C and Psaltis D 2012 *Opt. Express* **20** 10583
[13] Papadopoulos I N, Salma F, Christophe M and Psaltis D 2013 *Opt. Express* **4** 260
[14] Papadopoulos I N, Simandoux O, Farahi S, Huignard J P, Bossy E, Psaltis D and Moser C 2013 *Appl. Phys. Lett.* **102** 211106
[15] Czarske J W, Haufe D, Koukourakis N and Buttner L 2016 *Opt. Express* **24** 15128
[16] Ma C, Di J, Li Y, Xiao F, Zhang J, Liu K, Bai X and Zhao J 2018 *Appl. Phys. Express* **11** 062501
[17] Zuo H, Yang Z, Fang L and Luo S 2018 *Laser Phys.* **28** 096202
[18] Sivankutty S, Andresen E R, Cossart R, Bouwmans G, Monneret S and Rigneault H 2016 *Opt. Express* **24** 825
[19] N'Gom M, Norris T B, Michielssen E and Nadakuditi R R 2018 *Opt. Lett.* **43** 419
[20] Mahalati R N, Gu R Y and Kahn J M 2013 *Opt. Express* **21** 1656
[21] Papadopoulos I N, Farahi S, Moser C and Psaltis D 2013 *Opt. Lett.* **38** 2776
[22] Ploeschner M and Cizmar T 2015 *Opt. Lett.* **40** 197
[23] Bianchi S, Rajamanickam V P, Ferrara L, Fabrizio E D, Liberale C and Leonardo R D 2013 *Opt. Lett.* **38** 4935
[24] Loterie D, Farahi S, Papadopoulos I N, Goy A, Psaltis D and Moser C 2015 *Opt. Express* **23** 23845
[25] Laporte G P J, Stasio N, Moser C and Psaltis D 2015 *Opt. Express* **23** 27484
[26] Loterie D, Goorden S A, Psaltis D and Moser C 2015 *Opt. Lett.* **40** 5754
[27] Choi Y, Yoon C, Kim M, Yang J and Choi W 2013 *Opt. Lett.* **38** 2253
[28] Jang H, Yoon C, Chung E, Yang J and Choi W 2015 *Opt. Express* **23** 6705
[29] Popoff S M, Lerosey G, Carminati R, Fink M, Boccara A C and Gigan S 2010 *Phys. Rev. Lett.* **104** 100601
[30] Popoff S M, Lerosey G, Fink M, Boccara A C and Gigan S 2011 *New J. Phys.* **13** 123021
[31] Yamaguchi I and Zhang T 1997 *Opt. Lett.* **22** 1268
[32] Schreier P J and Scharf L L 2010 *Statistical Signal Processing of Complex-Valued Data: the Theory of Improper and Non-circular Signals* (Cambridge: Cambridge University Press) pp 85–8